

Ab Initio Study of the *Hypercloso* Boron Hydrides B_nH_n and $B_nH_n^-$. Exceptional Stability of Neutral $B_{13}H_{13}$

Michael L. McKee,^{*,†} Zhi-Xiang Wang,[‡] and Paul von Ragué Schleyer^{*,‡,§}

Contribution from the Department of Chemistry, Auburn University, Auburn, Alabama 36849, Computational Chemistry Annex, University of Georgia, Athens, Georgia 30602, and Computer Chemistry Center, Institut für Organische Chemie, Universität Erlangen-Nürnberg, Henkestrasse 42, D-91054 Erlangen, Germany

Received December 23, 1999. Revised Manuscript Received March 8, 2000

Abstract: The neutral *hypercloso* boron hydrides B_nH_n ($n = 5-13, 16, 19, 22$) and the boron hydride radical monocation $B_nH_n^+$ ($n = 5-13$) have been studied at the B3LYP/6-31G* and higher levels of density functional theory. The pairing and capping principles help rationalize the lowest energy structures. Neutral boron hydrides B_nH_n with $n = 3p + 1$ ($p = 2-7$) all have one boron atom on a 3-fold axis. Loss of one electron from $B_nH_n^{2-}$ ($n = 5-13$) is predicted to be exothermic except for $B_{12}H_{12}^{2-}$. This, the most stable and aromatic dianion, has a 10.9 kcal/mol (B3LYP/6-311+G**//B3LYP/6-31G*) adiabatic ionization potential. The relative stabilities of the neutral and monocation boron hydrides were evaluated using the equation $B_2H_2^x + (n - 2)BH_{inc} \rightarrow B_nH_n^x$, in which $x = 0$ and -1 and BH_{inc} is the energy difference between B_3H_5 (C_{2v} , planar) and B_2H_4 (D_{2h}). Removing two electrons from aromatic dianions changes the nucleus-independent chemical shifts (NICS) from negative (aromatic) to positive (antiaromatic) except for neutral B_6H_6 , B_7H_7 , $B_{12}H_{12}$ (C_{2v}), and $B_{13}H_{13}$ (C_{3v} , C_{2v} , C_s). The NICS values (ca. -21.0 ppm) for the three neutral $B_{13}H_{13}$ forms are comparable with the $B_{13}H_{13}^{2-}$ dianion value (-23.3 ppm). Interestingly, for all these species, the NICS values at points 1.0 Å above the centers of the unique triangles are all negative, which is in contrast to the case for benzene with well-known shielding and deshielding regions. On the basis of the stabilization energy and other aromatic criteria, the neutral $B_{13}H_{13}$ boron hydride appears to be a good candidate for synthesis.

Introduction

Boron hydrides can be placed into groups according to the number of electron pairs associated with cage bonding.¹ The designations are *closo*, *nido*, and *arachno* for cages with $n + 1$, $n + 2$, and $n + 3$ cage electron pairs, where n is the number of vertexes. In general, as the number of electron pairs increases for a cage, the structure becomes more open. Cages with fewer than $n + 1$ electron pairs are called *hypercloso*²⁻⁴ and generally fall into two categories: metalloboranes and metallocarboranes and boron halides (B_nX_n).⁷⁻¹¹ One

or more metal atoms in vertex positions may stabilize the unusual electron count in *isocloso* metalloboranes. In the boron halides (B_nX_n), the cage adopts a *closo* structure even though there are only n cage electron pairs rather than the required $n + 1$. The usual explanation is that the *exo* halide substituent supplies additional electron density to the cage through π back-donation. Boron halide cages (B_nX_n) are available for $n = 4, 7-12$. However, X-ray structures are known only for B_4X_4 , B_8X_8 , B_9X_9 , and $B_{11}X_{11}$. Mulvey et al.¹² calculated the bonding/antibonding nature of the HOMO in the boron hydride dianion and successfully predicted changes in the cage geometry between the dianion and the boron halide for cage sizes of $n = 8, 9$, and 11 (for more detail see individual discussions of B_8H_8 , B_9H_9 , and $B_{11}H_{11}$ below).

Porterfield et al.¹³ calculated the neutral boron hydrides B_nH_n ($n = 3-12$) and found distortions for $n = 3, 5, 6, 10$, and 12 from the regular deltahedral structures favored for the dianions $B_nH_n^{2-}$ due to the presence of an incompletely filled degenerate orbital level. For $n = 4, 8$, and 9, the $B_nH_n^{2-}$ HOMOs (e, b_2, a_2' symmetries, respectively) were computed to be nearly nonbonding; these three systems correspond to the boron halide clusters of greatest stability.

The PRDDO calculations of Bicerano, Marynick, and Lipscomb^{14,15} on larger boron hydride clusters ($n > 12$) found that

[†] Auburn University.

[‡] University of Georgia.

[§] Universität Erlangen-Nürnberg.

(1) (a) O'Neill, M. E.; Wade, K. *THEOCHEM* **1983**, *103*, 259. (b) O'Neill, M. E.; Wade, K. *Polyhedron* **1984**, *3*, 199. (c) Mingos, D. M. P.; Wales, D. J. *Introduction to Cluster Chemistry*; Prentice Hall: Englewood Cliffs, NJ, 1990.

(2) (a) Baker, R. T. *Inorg. Chem.* **1986**, *25*, 109. (b) Kennedy J. D. *Inorg. Chem.* **1986**, *25*, 111. (c) Kennedy, J. D. *Disobedient Skeletons. In The Borane, Carborane, Carbocation Continuum*; Casanova, J., Ed.; Wiley: New York, 1998; pp 85–116.

(3) Johnston, R. L.; Mingos, D. M. P. *Inorg. Chem.* **1986**, *25*, 3321.

(4) McKee, M. L. *Inorg. Chem.* **1999**, *38*, 321.

(5) (a) *Advances in Boron Chemistry*; Siebert, W., Ed.; Royal Society of Chemistry: Cambridge, 1997. (b) *The Borane, Carborane, Carbocation Continuum*; Casanova, J., Ed.; Wiley: New York, 1998.

(6) (a) Johnston, R. L.; Mingos, D. M. P.; Sherwood, P. *New J. Chem.* **1991**, *15*, 831. (b) Bould, J.; Rath, N. P.; Barton, L. *Organometallics* **1995**, *14*, 2119. (c) Lei, X.; Shang, M.; Fehlner, T. P. *Inorg. Chem.* **1998**, *37*, 3900. (d) Weller, A. S.; Shang, M.; Fehlner, T. P. *Organometallics* **1999**, *18*, 853.

(7) Morrison, J. A. *Chem. Rev.* **1991**, *91*, 35.

(8) King, R. B. *Inorg. Chem.* **1999**, *38*, 5151.

(9) LeBreton, P. R.; Urano, S.; Shahbaz, M.; Emery, S. L.; Morrison, J. A. *J. Am. Chem. Soc.* **1986**, *108*, 3937.

(10) Swanton, D. J.; Ahlrichs, R.; Häser, M. *Chem. Phys. Lett.* **1989**, *155*, 329.

(11) Hönle, W.; Grin, Y.; Burkhardt, A.; Wedig, U.; Schultheiss, M.; von Schnering, H. G. *J. Solid State Chem.* **1997**, *133*, 59.

(12) Mulvey, R. E.; O'Neill, M. E.; Wade, K. *Polyhedron* **1986**, *5*, 1437.

(13) Porterfield, W. W.; Jones, M. E.; Gill, W. R.; Wade, K. *Inorg. Chem.* **1990**, *29*, 2914.

closed-shell high-symmetry structures were possible for the neutral deltahedral cages of 16, 19, and 22 vertexes but not for the corresponding dianions (which would have degenerate orbitals partially occupied). Schleyer and co-workers evaluated the stability of the $B_{13}H_{13}^{2-}$ dianion as well as the $B_{14}H_{14}^{2-}$ through $B_{17}H_{17}^{2-}$ series recently.¹⁶ Lipscomb et al. have computed selected boron hydride dianions as large as $B_{36}H_{36}^{2-}$ as well as extensions into boron nanotubes.¹⁷ A very significant breakthrough has been reported by Gaines and co-workers,¹⁸ who synthesized $B_{19}H_{19}^{2-}$, the first observed *closo* boron hydride dianion larger than $B_{12}H_{12}^{2-}$.

We wish to answer several questions: (1) What are the geometries and electronic structures of the neutral and radical anion cages? (2) Are the boron hydride dianions stable to loss of an electron (vertical and adiabatic)? (3) Do neutral boron hydrides B_nH_n and boron hydride radical anions $B_nH_n^-$ show characteristics of aromaticity? (4) Are there neutral and radical anion cages with high stability?

Morrison⁷ suggested that 7-, 10-, and 12-atom boron halide (B_nX_n) may not adopt normal *closo* structures, but rather “a separate series of deltahedra, the ‘hypercloso’ structures”. Indeed, $[(\eta^6\text{-MeC}_6\text{H}_4\text{CHMe}_2)\text{RuB}_9\text{H}_9]$, a 10-vertex *hypercloso* metalloborane, is known to have a quite different geometry than the $B_{10}H_{10}^{2-}$ D_{4d} symmetry structure.^{2a}

Few boron hydride $B_nH_n^-$ (or boron halide $B_nX_n^-$) radical anions have been characterized.^{19,20} One example is $B_8H_8^-$, which is synthesized by oxidative degradation of $B_9H_9^{2-}$ (eq 1).²⁰ On the ESR time scale, all boron and hydrogen atoms are



equivalent and coupled to the odd electron equally. An analysis of the ESR spectrum²⁰ gave the following isotropic hyperfine coupling constants (HFCCs, in gauss): $a_{\text{HFCC}}(^1\text{H}) = 6.10$; $a_{\text{HFCC}}(^{11}\text{B}) = 2.52$; $a_{\text{HFCC}}(^{10}\text{B}) = 0.84$. A dodecahedral $B_8H_8^-$ structure (D_{2d} symmetry) has two sets of four equivalent boron and hydrogen positions. The equivalency of boron and hydrogen positions observed by ESR could be due to similar a_{HFCC} values for the two sets of positions or too fast an equilibration process on the ESR time scale. The possibility of a static square antiprism (D_{4d}) for the radical anion can be discounted because the electronic state would be degenerate and would Jahn–Teller distort to a lower symmetry structure.

(14) Bicerano, J.; Marynick, D. S.; Lipscomb, W. N. *Inorg. Chem.* **1978**, *17*, 2041.

(15) Bicerano, J.; Marynick, D. S.; Lipscomb, W. N. *Inorg. Chem.* **1978**, *17*, 3443.

(16) (a) Yang, X.; Jiao, H.; Schleyer, P. v. R. *Inorg. Chem.* **1997**, *36*, 4897. (b) Schleyer, P. v. R.; Najafian, K.; Mebel, A. M. *Inorg. Chem.* **1998**, *37*, 6765.

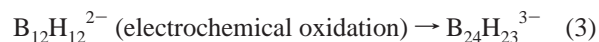
(17) (a) Gindulyt, A.; Lipscomb, W. N.; Massa, L. *Inorg. Chem.* **1998**, *37*, 6544. (b) Gindulyt, A.; Krishnamachari, N.; Lipscomb, W. N.; Massa, L. *Inorg. Chem.* **1998**, *37*, 6546.

(18) Dopke, J. A.; Powell, D. R.; Gaines, D. F. *Inorg. Chem.* **2000**, *39*, 463.

(19) (a) Muetterties, E. L.; Knoth, W. H. *Polyhedral Boranes*; Marcel Dekker: New York, 1968. (b) Fowler, P. W. *J. Chem. Soc., Faraday Trans. 2* **1986**, *82*, 61. (c) $B_6X_6^-$: Heinrich, A.; Keller, H.-L.; Preetz, W. *Z. Naturforsch.* **1990**, *45b*, 184. (d) $B_6X_6^-$: Lorenzen, L.; Preetz, W. *Z. Naturforsch.* **1997**, *52b*, 565. (e) $B_6X_6^-$: Lorenzen, V.; Preetz, W.; Baumann, F.; Kaim, W. *Inorg. Chem.* **1998**, *37*, 4011. (f) $B_9X_9^-$: Wong, E. H.; Kabbani, R. M. *Inorg. Chem.* **1980**, *19*, 451. (g) $B_{10}H_{10}^-$: Lewis, J. S.; Kaczmarczyk, A. *J. Am. Chem. Soc.* **1966**, *88*, 1068. (h) $B_8X_8^-$ and $B_9X_9^-$: Speiser, B.; Tittel, C.; Einholz, W.; Schäfer, R. *J. Chem. Soc., Dalton Trans.* **1999**, 1741.

(20) Klanberg, F.; Eaton, D. R.; Guggenberger, L. J.; Muetterties, E. L. *Inorg. Chem.* **1967**, *6*, 1271.

Electrochemical oxidation of both $B_{10}H_{10}^{2-}$ and $B_{12}H_{12}^{2-}$ (eqs 2 and 3) is likely to proceed through formation of the radical anion as the first step.^{21,22} The $B_{20}H_{19}^{3-}$ and $B_{24}H_{23}^{3-}$ structures are believed to be double cages connected by apical–equatorial B–H–B bridges.^{21–23}



Michl and co-workers²⁴ have generated a stable radical $CB_{11}Me_{12}$ in which the cage is “sheaved” by a layer of methyl groups. The radical, which is isoelectronic with $B_{12}H_{12}^-$, persists in air for a few days and at 150 °C. A broad ESR signal was observed in solution and low-temperature glasses. A computational study²⁵ of CB_9H_{10} and $CB_{11}H_{12}$ found that the symmetries of the anion were lowered due to the Jahn–Teller effect to C_{2v} (from C_{4v}) and C_s (from C_{5v}), when an electron was removed from $CB_9H_{10}^-$ and $CB_{11}H_{12}^-$, respectively. The $B_{12}Me_{12}^-$ radical ion has recently been reported by Hawthorne and co-workers,²⁶ who made the air-stable anion by oxidizing $B_{12}Me_{12}^{2-}$ with ceric (IV) ammonium nitrate in acetonitrile.

Computational Methods

All geometries were fully optimized in the given symmetry at the B3LYP/6-31G(d) level.^{27a,b} Vibrational frequencies, calculated at that level, determined the nature of the stationary points. Single-point energies at B3LYP/6-311+G(d)//B3LYP/6-31G(d) constitute the “standard” level. Zero-point corrections are very small and have not been included unless specifically noted.

The B3LYP/6-31G(d) geometries for boranes and carboranes have been shown to be accurate and comparable to those at MP2/6-31G(d).^{27c} Molecular plots of the relevant structures are given in Figures 1. Tables of total energies (hartrees) and zero-point energies (kcal/mol) as well as Cartesian coordinates of all species are provided as Supporting Information.

Results and Discussion

The molecular symmetries of the boron hydride dianions are well established. In contrast, little is known about the molecular

(21) Midaugh, R. L.; Wiersema, R. J. *J. Am. Chem. Soc.* **1966**, *88*, 4147.

(22) Wiersema, R. J.; Midaugh, R. L. *J. Am. Chem. Soc.* **1967**, *89*, 5078.

(23) Mebel, A. M.; Najafian, K.; Charkin, O. P.; Schleyer, P. v. R. *THEOCHEM* **1999**, *461–462*, 187.

(24) (a) King, B. T.; Janoušek, Z.; Grüner, B.; Trammell, M.; Noll, B. C.; Michl, J. *J. Am. Chem. Soc.* **1996**, *118*, 3313. (b) King, B. T.; Noll, B. C.; McKinley, A. J.; Michl, J. *J. Am. Chem. Soc.* **1996**, *118*, 10902.

(25) McKee, M. L. *J. Am. Chem. Soc.* **1997**, *119*, 4220.

(26) Peymann, T.; Knobler, C. B.; Hawthorne, M. F. *Chem. Commun.* **1999**, 2039.

(27) (a) Frisch, M. J.; Trucks, G. W.; Schlegel, H. B.; Gill, P. M. W.; Johnson, B. G.; Robb, M. A.; Cheeseman, J. R.; Keith, T.; Petersson, G. A.; Montgomery, J. A.; Raghavachari, K.; Al-Laham, M. A.; Zakrzewski, V. G.; Ortiz, J. V.; Foresman, J. B.; Cioslowski, J.; Stefanov, B. B.; Nanayakkara, A.; Challacombe, M.; Peng, C. Y.; Ayala, P. Y.; Chen, W.; Wong, M. W.; Andres, J. L.; Replogle, E. S.; Gomperts, R.; Martin, R. L.; Fox, D. J.; Binkley, J. S.; Defrees, D. J.; Baker, J.; Stewart, J. P.; Head-Gordon, M.; Gonzalez, C.; Pople, J. A. *Gaussian 94*; Gaussian, Inc.: Pittsburgh, PA, 1995. (b) Frisch, M. J.; Trucks, G. W.; Schlegel, H. B.; Scuseria, G. E.; Robb, M. A.; Cheeseman, J. R.; Zakrzewski, V. G.; Montgomery, J. A., Jr.; Stratmann, R. E.; Burant, J. C.; Dapprich, S.; Millam, J. M.; Daniels, A. D.; Kudin, K. N.; Strain, M. C.; Farkas, O.; Tomasi, J.; Barone, V.; Cossi, M.; Cammi, R.; Mennucci, B.; Pomelli, C.; Adamo, C.; Clifford, S.; Ochterski, J.; Petersson, G. A.; Ayala, P. Y.; Cui, Q.; Morokuma, K.; Malick, D. K.; Rabuck, A. D.; Raghavachari, K.; Foresman, J. B.; Cioslowski, J.; Ortiz, J. V.; Stefanov, B. B.; Liu, G.; Liashenko, A.; Piskorz, P.; Komaromi, I.; Gomperts, R.; Martin, R. L.; Fox, D. J.; Keith, T.; Al-Laham, M. A.; Peng, C. Y.; Nanayakkara, A.; Gonzalez, C.; Challacombe, M.; Gill, P. M. W.; Johnson, B.; Chen, W.; Wong, M. W.; Andres, J. L.; Head-Gordon, M.; Replogle, E. S.; Pople, J. A. *Gaussian 98*; Gaussian, Inc.: Pittsburgh, PA, 1998. (c) See: *The Encyclopedia of Computational Chemistry*; Schleyer, P. v. R., Allinger, N. L., Clark, T., Gasteiger, J., Kollman, P. A., Schaefer, H. F., III, Schreiner, P. R., Eds.; John Wiley & Sons: Chichester, 1998.

symmetries of the radical monoanion and neutral boron hydrides, B_nH_n⁻ and B_nH_n. Since several of the boron hydride dianions have degenerate HOMOs, removing an electron creates an electronic state which will Jahn–Teller distort.¹³ The following procedure was used to determine the direction of distortion. First, the radical anion was optimized at the AM1 level²⁸ in the point group of the dianion, and vibrational frequencies were calculated. The molecule was distorted along the vector with the most negative eigenvalue and reoptimized. This geometry was used as the initial guess for the B3LYP/6-31G(d) optimization. If an imaginary frequency was found at the B3LYP/6-31G(d) level, the optimization was repeated in a lower point group until a minimum was found. When a stationary point was close to a symmetry higher than that assumed, the higher symmetry point group was used and the geometry reoptimized. We considered different structures for several of the radical monoanions and neutral boron hydrides but were unable to find structures of lower energy than those given by the procedure above.

In a recent paper, King²⁹ considered distortions from idealized symmetries in transition metal complexes when the orbital degeneracy was lifted. We find a close parallel with our results and his predictions for trigonal bipyramidal, octahedral, and pentagonal bipyramid complexes. We find symmetry changes from D_{3h} to C_{2v} to C_{4v} when one and two electrons are removed from B₅H₅²⁻. Similarly, the symmetry changes from O_h to D_{3d} to C_{2v} when one and two electrons are removed from B₆H₆²⁻. Finally, the symmetry of B₇H₇²⁻ changes from D_{5h} to C_s to C_{3v} when one and two electrons are removed. King predicted similar distortions in five-, six-, and seven-coordinate transition metal complexes.

In analyzing the structures of the neutral boron hydride, it is useful to consider the pairing principle^{1,30} and the capping principle.^{1,31} The pairing principle states that if a structure has one boron on a 3-fold axis or higher, then degenerate bonding and antibonding orbitals will be paired except for one degenerate set which will be nonbonding. A *closo* electron count ($n + 1$ electron pairs) would give an open-shell system in which the degenerate nonbonding orbitals are partially filled. However, either an electron count of n or $n + 2$ electron pairs would give a closed-shell species. The simplest boron hydride with one boron on a 3-fold axis and an n electron pair count is B₄H₄ in T_d symmetry. Additional members of this series have $3p + 1$ vertex positions, i.e., B_nH_n, $n = 7, 10, 13, 16, 19, 22$, and so on.

The capping principle states that a capped polyhedral cluster has the same number of bonding skeletal molecular orbitals as the uncapped polyhedron. Thus, a polyhedron of n vertexes and having $n + 1$ bonding molecular orbitals (*closo* electron count) can accept a capping vertex without changing the number of bonding molecular orbitals. Therefore, the boron hydrides might prefer a structure in which a BH group caps the next smaller polyhedral cage. Indeed, this behavior is observed for all the neutral boron hydrides derived from dianions having degenerate HOMOs as well as B₁₃H₁₃ in which the HOMO of the dianion is not degenerate (Table 1). In Figure 1, an additional picture of the neutral boron hydride is given which emphasizes the capping of the next smaller polyhedron.

We will first discuss properties of the individual boron hydride cages followed by a discussion of trends.

Table 1. Summary of Properties of Dianion and Neutral Boron Hydrides

vertex	dianion boron hydride				neutral boron hydride		
	symm	highest n -fold ^a	atoms on n -fold ^b	degen HOMO?	type of distort. ^c	symm	H–L gap ^d
5	D _{3h}	3	2	yes	DSD	C _{4v}	101.0
6	O _h	4	2	yes	DSD	C _{2v}	109.5
7	D _{5h}	5	2	yes	DSD	C _{3v}	125.0
8	D _{2d}	2	0	no	none	D _{2d}	90.2
9	D _{3h}	3	0	no	none	D _{3h}	88.0
10	D _{4d}	4	2	yes	DSD	C _{3v}	110.2
11	C _{2v}	2	1	no	none	C _{2v}	81.4
12	I _h	5	2	yes	DSD	C _{2v}	88.9
13	C _{2v}	2	1	no	cap ^e	C _{3v}	144.9

^a Refers to the principal axis of the dianion. ^b Number of boron atoms on highest n -fold axis. ^c Type of distortion the dianion undergoes when two electrons are removed. DSD refers to a diamond–square–diamond distortion. ^d HOMO–LUMO gap in the neutral boron hydride in kcal/mol. ^e The neutral B₁₃H₁₃ cage undergoes a distortion to a capping geometry.

B₅H₅. Removing one electron from B₅H₅²⁻ increases one of the equatorial B–B distances to 1.963 Å. Removing the second electron increases the B–B distance to 2.394 Å to give a neutral boron hydride with C_{4v} symmetry. The capping principle suggests that B₅H₅ might be stabilized by adopting the structure of the B₄H₄ *closo* cage with a BH capping group, i.e., a capped tetrahedron. However, the underlying four-vertex cage is not expected to be stable in a tetrahedral geometry with $n + 1$ electron pairs owing to the incompletely filled degenerate orbitals. A better way to view the B₅H₅ structure is from the pairing principle. A single boron atom is located on the 4-fold axis which leads to five cage-bonding orbitals, five cage-antibonding orbitals, and a pair of nonbonding orbitals (in general, for an n -vertex cage with one boron atom on a 4-fold axis, there are n bonding, n antibonding and two nonbonding orbitals). A stable structure results when all of the cage bonding orbitals are filled.

It is also interesting to note that the diamond–square–diamond (DSD) rearrangement of B₅H₅²⁻ is symmetry forbidden³² owing to a crossing of occupied and unoccupied orbitals along the reaction path. Removing two electrons removes the forbidden character of the reaction, and the transformation is actually downhill from the trigonal bipyramid to the square pyramid. It should also be pointed out that a B₅H₅ isomer exists lower in energy than the C_{4v} structure. The B₅H₅ global minimum is a C_s structure with a central aromatic BBB ring 9.8 kcal/mol more stable than the square pyramid at B3LYP/6-31G(d)//B3LYP/6-31G(d).⁴

B₆H₆. When an electron is removed from the HOMO of B₆H₆²⁻ (t_{2g} symmetry), a number of different distortions are possible. Following the procedure outlined above, we first found a ²B_{3g} state of D_{2h} symmetry, where the symmetry of t_{2g} orbitals is split into a_g, b_{1g}, and b_{3g}. Following the imaginary frequency of the D_{2h} structure leads to a ²A_{1g} state of D_{3d} symmetry (D_{2h} → C_{2h}; then symmetrized to D_{3d}) 1.2 kcal/mol lower in energy, where the symmetry of the original t_{2g} orbitals (in O_h symmetry) has divided into a_{1g} and e_g orbitals. Removing an electron from the radical anion leads to a neutral B₆H₆ boron hydride with C_{2v} symmetry and no imaginary frequencies. The structure closely resembles a capped trigonal bipyramid (Figure 1).

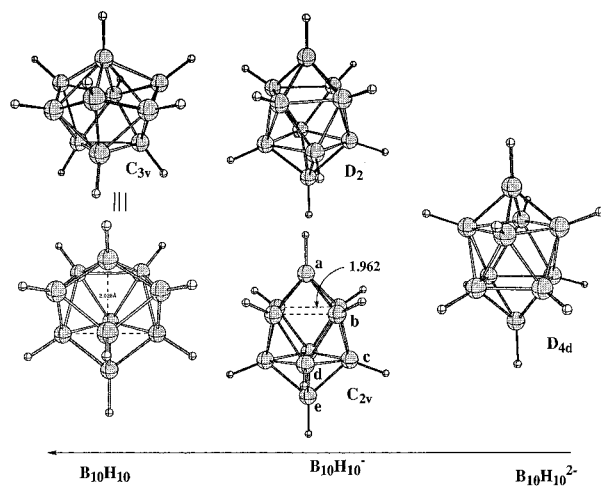
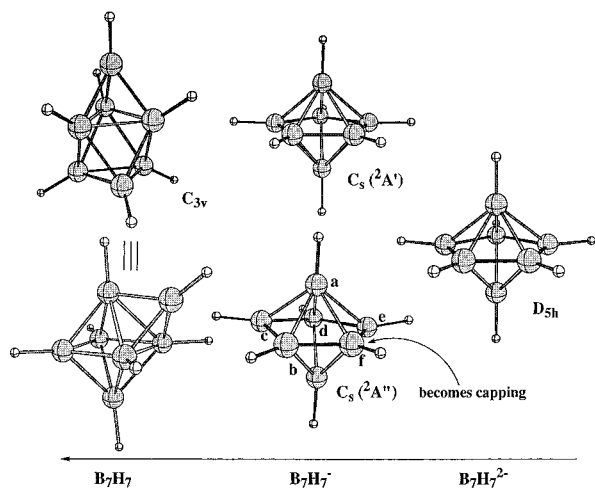
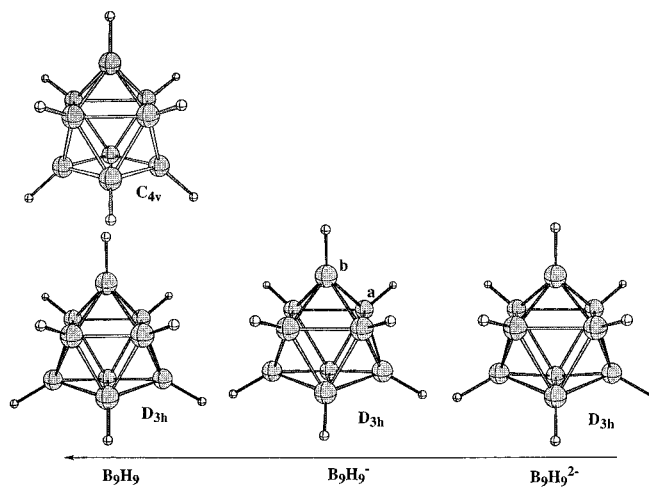
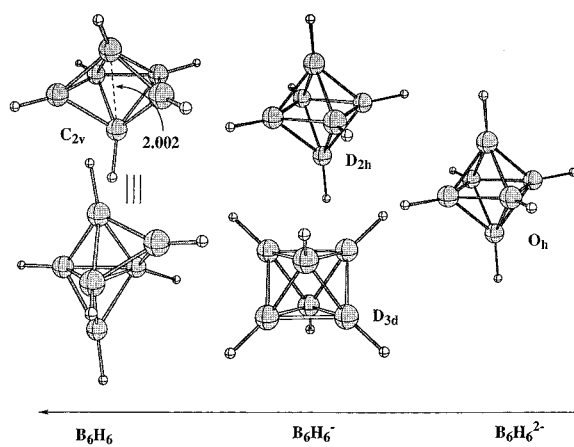
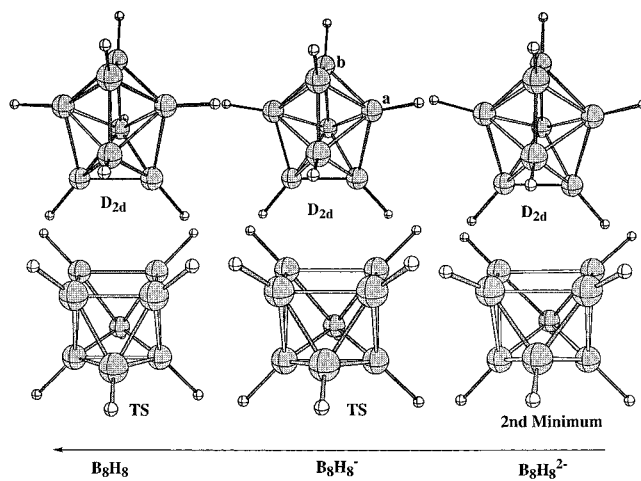
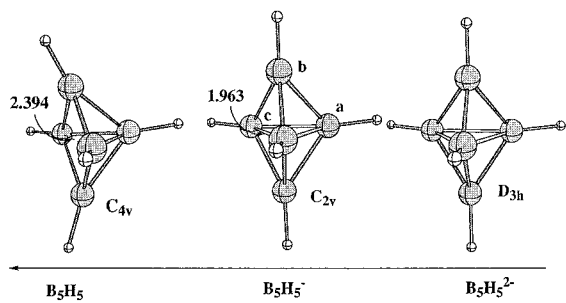
(28) Dewar, M. J. S.; Zoebisch, E. G.; Healy, E. F.; Stewart, J. J. P. *J. Am. Chem. Soc.* **1985**, *107*, 3902.

(29) King, R. B. *Inorg. Chim. Acta* **1998**, *270*, 68.

(30) Fowler, P. W. *Polyhedron* **1985**, *4*, 2051.

(31) Mingos, D. M. P.; Forsyth, M. I. *J. Chem. Soc., Dalton Trans.* **1977**, 610.

(32) Gimarc, B. M.; Ott, J. J. Graphs for Chemical Reaction Networks: Application to the Carboranes. In *Graph Theory and Topology in Chemistry*; King, R. B., Rouvray, D. H., Eds.; Elsevier: Amsterdam, 1987; pp 285–301.



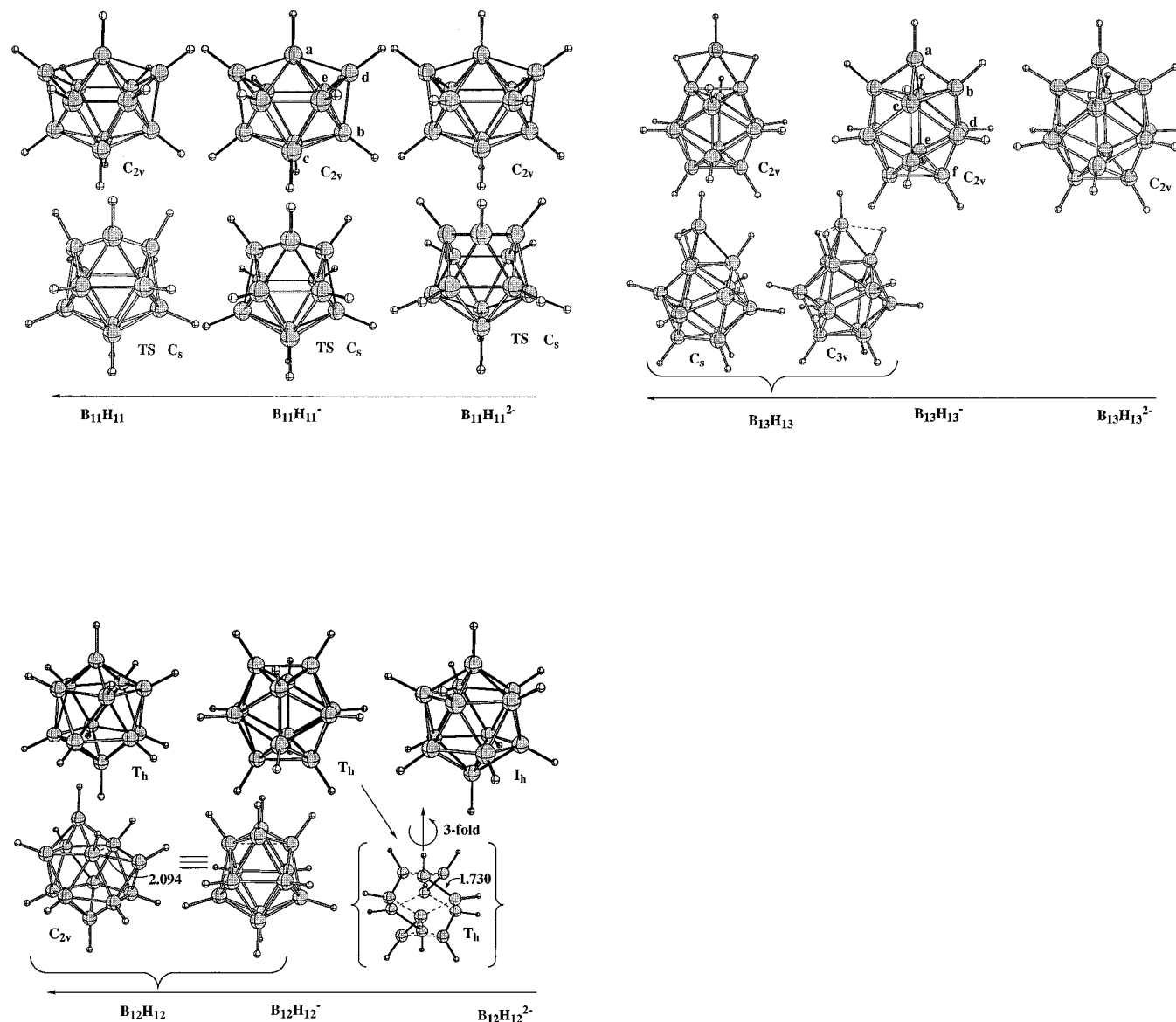


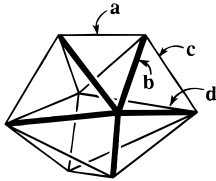
Figure 1. Molecular plots for neutral, radical anion, and dianion boron hydride cages. The arrow at the bottom of each vertex group indicates the ionization sequence for removing one and two electrons from the dianion. In several plots a second view of the neutral boron hydride is given to illustrate the relationship with the next smaller *closo* boron hydride dianion. The letters adjacent to the boron atoms of the radical anion correspond to column headings in Table 7. The second view of the $B_{12}H_{12}^-$ radical is included to show the 3-fold axis. The six B–B distances shown (1.730 Å) make up a complete set. All other B–B bonding distances are 1.819 Å.

$B_7H_7^-$. Two states of the $B_7H_7^-$ radical anion were obtained in C_s symmetry depending on the location of the molecular plane. In one cage, a molecular plane passes through the two axial boron atoms to produce a ${}^2A'$ electronic state, while in the other cage, the molecular plane passes through the five equatorial boron atoms (${}^2A''$ state). The ${}^2A'$ state is a stationary point with two imaginary frequencies, one of which leads to the ${}^2A''$ state, 0.3 kcal/mol lower in energy at the B3LYP/6-311+G(d)//B3LYP/6-31G(d) level. However, when zero-point corrections are added, the stability order reverses by 0.6 kcal/mol. We chose to refer to the ${}^2A''$ state as the ground state because the reversal is mainly due to the contribution (or rather the lack of contribution) from the two imaginary frequencies to the zero-point energy. If the ${}^2A'$ state were the ground state, then these two modes should contribute to the ZPE. In such cases, the harmonic approximation is not appropriate.

When an electron is removed from the ${}^2A''$ radical anion, a neutral B_7H_7 cage is obtained with C_{3v} symmetry. Essentially,

two boron atoms which were nonadjacent in the pentagonal bipyramid have bonded while the vertex between these two positions assumes a capping position, forming a capped octahedron (Figure 1).

$B_8H_8^-$. The b_2 HOMO of D_{2d} $B_8H_8^{2-}$ is nondegenerate, so removing an electron does not necessarily lead to a symmetry lowering. Indeed, the lowest energy structure located on the $B_8H_8^-$ potential energy surface (PES) was the 2B_2 state in D_{2d} symmetry. Since $B_8H_8^-$ is the only boron hydride radical anion to be characterized by ESR,²⁰ we have computed isotropic hyperfine coupling constants (HFCCs) for ${}^{11}B$ and 1H (B3LYP/6-311+G(d)//B3LYP/6-31G(d)). In D_{2d} symmetry, there are two sets of boron and hydrogen atoms ("a" and "b", see Figure 1). For sets "a" and "b", the $a_{HFCC}({}^{11}B)$ values are -4.8 and $+1.9$ G, respectively, while the $a_{HFCC}({}^1H)$ values are -5.5 and $+13.6$ G, respectively. In the experimental ESR spectrum (sign not determined),²⁰ only one HFCC value is observed for the electron coupling to boron ($a_{HFCC}({}^{11}B) = 2.52$ G) and to hydrogen

Table 2. Calculated and Experimental Distances in B_8H_8 Cages


	"a"	"b"	"c"	"d"
X-ray $B_8H_8^{2-}$ ^a	1.559	1.756	1.717	1.926
X-ray $B_8Cl_8^{a,b}$	1.681	1.744	1.814	2.001
	(0.122)	(-0.012)	(0.097)	(0.075)
$B_8H_8^{2-}$	1.617	1.821	1.708	1.909
$B_8H_8^{-c}$	1.661	1.775	1.734	1.909
	(0.044)	(-0.046)	(0.026)	(0.000)
$B_8H_8^c$	1.751	1.742	1.753	1.925
	(0.134)	(-0.079)	(0.045)	(0.016)

^a See ref 12. ^b The numbers in parentheses represent the bond length difference between B_8Cl_8 and $B_8H_8^{2-}$. ^c The numbers in parentheses represent the bond length difference between $B_8H_8^-/B_8H_8$ and $B_8H_8^{2-}$.

($a_{HFCC}(^1H) = 6.1$ G). Because a higher symmetry structure and the accidental equivalence of the HFCC values could be ruled out, the authors suggested²⁰ that the D_{2d} structure was undergoing rapid rearrangement.

We considered the possibility that the radical anion might go through the same mechanism as the $B_8H_8^{2-}$ dianion, which is known to undergo rapid rearrangement on the NMR time scale.^{33,34} Bühl et al.³³ calculated a 5.0 kcal/mol barrier for rearrangement via a DSD mechanism in the dianion at the MP2/6-31G(d)//6-31G(d)+ZPC level. At the B3LYP/6-311+G(d)//B3LYP/6-31G(d)+ZPC level, we find the C_{2v} $B_8H_8^{2-}$ structure (a minimum at B3LYP/6-31G(d)) to be 2.6 kcal/mol higher than the D_{2d} structure. This should be close to the activation barrier. The corresponding energy differences (C_{2v} vs D_{2d}) are 7.7 kcal/mol for the radical anion, and 8.2 kcal/mol for the neutral B_8H_8 . Note that C_{2v} structures were characterized as transition states (one imaginary frequency) for both $B_8H_8^-$ and B_8H_8 at the B3LYP/6-31G(d) level.

If the rearrangement is fast on the ESR time scale, then the average calculated ESR parameters would be $a_{HFCC}(^{11}B) = 1.4$ G and $a_{HFCC}(^1H) = 4.0$ G. These compare satisfactorily with the experimental values of 2.52 and 6.1 G, respectively.

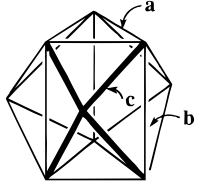
The geometric consequences of removing two electrons from the dianion can be ascertained by comparing X-ray structures of $B_8H_8^{2-}$ and B_8Cl_8 . As summarized in Table 2, distances "a", "c", and "d" all increase when two electrons are removed while distance "b" decreases. It is reasonable that the cage should expand since electrons are removed from a skeletal bonding molecular orbital. The B3LYP/6-31G(d) calculated bond changes are in reasonable agreement with experiment, both in sign (increase or decrease) and in magnitude. Note that the radical anion bond distances are intermediate between those of the dianion and the neutral boron hydride (Table 2).

B_9H_9 . Since the HOMO of $B_9H_9^{2-}$ is nondegenerate (a_2' symmetry), the radical anion may be stable in the same D_{3h} point group. Indeed, not only is the $^2A_2'$ $B_9H_9^-$ state calculated to be a minimum in D_{3h} symmetry, but the same is also true of the neutral B_9H_9 boron hydride.

B_9H_9 is the second member of the $4p + 1$ p -vertex cage series (B_5H_5 is the first) which can have one boron atom lying on a 4-fold axis. While the C_{4v} structure is a minimum for B_5H_5 ,

(33) Bühl, M.; Mebel, A. M.; Charkin, O. P.; Schleyer, P. v. R. *Inorg. Chem.* **1992**, *31*, 3769.

(34) Bausch, J. W.; Prakash, G. K. S.; Williams, R. E. *Inorg. Chem.* **1992**, *31*, 3763.

Table 3. Calculated and Experimental Distances in B_9H_9 Cages


	"a"	"b"	"c"
X-ray $B_9H_9^{2-}$ ^a	1.91	1.84	1.71
X-ray $B_9Cl_9^{a,c}$	1.80	2.08	1.75
	(-0.11)	(0.24)	(0.04)
X-ray $B_9Cl_9^{b,c}$	1.800	2.057	1.740
	(-0.11)	(0.22)	(0.03)
$B_9H_9^{2-}$	1.986	1.791	1.711
$B_9H_9^{-d}$	1.870	1.896	1.728
	(-0.116)	(0.105)	(0.017)
$B_9H_9^d$	1.796	2.020	1.751
	(-0.196)	(0.229)	(0.040)

^a See ref 12. ^b Reference 11. ^c The numbers in parentheses represent the bond length difference between B_9Cl_9 and $B_9H_9^{2-}$. ^d The numbers in parentheses represent the bond length difference between $B_9H_9^-/B_9H_9$ and $B_9H_9^{2-}$.

the C_{4v} geometry of B_9H_9 offers the least-motion DSD interconversion of D_{3h} minima. The activation barrier is only 2.1 kcal/mol (including ZPE); hence, the neutral B_9H_9 cage should be fluxional, unlike that of $B_9H_9^{2-}$, which is quite rigid.³² It is possible that the degenerate rearrangement barrier in B_9Cl_9 also is small since the boron halide has an n -electron pair count. Very recent calculations³⁵ on $B_9H_9^{2-}$ show that the single DSD step has an activation barrier of 28.4 kcal/mol, while the double DSD step has a smaller barrier of 21.3 kcal/mol (B3LYP/6-311+G(d,p)//B3LYP/6-31G(d)+ZPC).

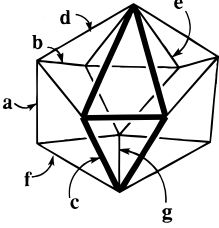
A comparison of the $B_9H_9^{2-}$ and B_9Cl_9 X-ray structures is given in Table 3. As electrons are removed from the cage ($B_9H_9^{2-} \rightarrow B_9Cl_9$), the distances in the two equilateral BBB triangles centered on the principal axis decrease (set "a"), while the separation between the two BBB faces increases (set "b"). The distances between the three capping boron atoms and the four boron atoms in the square faces remain similar (set "c"). These observations are closely modeled by the calculated distance changes (Table 3; $B_9H_9^{2-} \rightarrow B_9H_9^- \rightarrow B_9H_9$).

$B_{10}H_{10}$. Removing one electron from $B_{10}H_{10}^{2-}$ gave a $B_{10}H_{10}^{-2}B_1$ state in D_2 symmetry. In the middle tier of boron atoms, the four equivalent B-B distances (1.842 Å) in the C_{4v} dianion become 1.799 and 1.928 Å in the D_2 radical anion. Most of the unpaired spin density in the 2B_1 state resides on the two boron atoms on the 2-fold axis (formerly 4-fold), which is in keeping with the antipodal effect³⁶ (dianion HOMO has a large contribution from the axial boron). The D_2 $B_{10}H_{10}^-$ structure has one imaginary frequency which leads to a minimum in C_{2v} symmetry (2B_1 state), 0.1 kcal/mol lower in energy at the B3LYP/6-311+G(d)//B3LYP/6-31G(d) level. While zero-point correction reverses the ordering of the two states, we chose to consider the C_{2v} structure as the ground state for the same reason discussed above for $B_7H_7^-$.

In going from the D_2 to the C_{2v} $B_{10}H_{10}^-$ structure, the B-B distances of the second tier of four boron atoms become equal

(35) Mebel, A. M.; Schleyer, P. v. R.; Najafian, K.; Charkin, O. P. *Inorg. Chem.* **1998**, *37*, 1693.

(36) (a) Plešek, J.; Heřmánek, S. *J. Chem. Soc., Chem. Commun.* **1975**, 127. (b) Heřmánek, S.; Gregor, V.; Štíbr, B.; Plešek, J.; Janousek, Z.; Antonovich, V. A. *Collect. Czech. Chem. Commun.* **1976**, *41*, 1492. (c) Heřmánek, S.; Jelínek, T.; Plešek, J.; Štíbr, B.; Fusek, J.; Mareš, F. In *Boron Chemistry, Proceeding of the 6th IMEBORON*; Heřmánek, S., Ed.; World Scientific: Singapore, 1987; pp 26-73.

Table 4. Calculated and Experimental Distances in B₁₁H₁₁ Cages


	a	b	c	d	e	f	g
X-ray ^a	1.771	1.655	1.788	1.745	2.012	1.766	1.781
B ₁₁ H ₁₁ ²⁻	1.759	1.671	1.785	1.745	2.025	1.788	1.830
B ₁₁ H ₁₁ ⁻	1.742	1.702	1.783	1.772	1.998	1.794	1.788
B ₁₁ H ₁₁	1.739	1.730	1.785	1.836	1.946	1.796	1.772

^a X-ray of [B₁₁H₁₀SMe₂]⁻; see ref 12.

(Figure 1), while the differentiation of the B–B distances in the upper tier becomes larger (1.775 and 1.962 Å). The unpaired spin density remains largely on the two axial boron atoms. The *D*₂ transition state will result in equivalence of all eight boron atoms in the middle tiers of the *C*_{2*v*} structure. Thus, the ESR spectrum of B₁₀H₁₀⁻ should reveal two sets of boron atoms in the ratio of 2:8 (axial:equatorial). The predicted HFCC values are *a*_{HFCC}(¹¹B) = 1.6 and -1.8 G (2:8 ratio) and *a*_{HFCC}(¹H) = -6.0 and -0.6 G (2:8 ratio).

The B₁₀H₁₀⁻ radical may have been observed by Lewis and Kaczmarczyk^{19f} in the oxidation of B₁₀H₁₀²⁻ with CuCl₂. Also, B₁₀H₁₀⁻ is the likely intermediate in the oxidative coupling of B₁₀H₁₀²⁻.²¹

If an electron is removed from the B₁₀H₁₀⁻ *C*_{2*v*} structure, the 1.962 Å B–B distance increases to 2.912 Å while a boron atom in the lower tier moves up to assume a capping position over an open six-membered face: this results in a *C*_{3*v*} B₁₀H₁₀ neutral cage (Figure 1). Neutral B₁₀H₁₀ is the third member of the 3*p* + 1 *p*-vertex boron hydrides (B₄H₄ and B₇H₇ are the first and second). The single boron atom on the 3-fold axis ensures that the *n* electron pairs all go into maximally cage bonding orbitals (pairing principle). Johnston and Mingos³ used Hückel calculations to show that neutral B₁₀H₁₀ was more stable in *C*_{3*v*} symmetry than in the bicapped square antiprism (*D*_{4*d*}) arrangement.

B₁₁H₁₁. When the B₁₁H₁₁²⁻ dianion (*a*₂ symmetry HOMO) loses an electron, a radical ion of ²A₂ symmetry is produced. Further electron loss to form neutral B₁₁H₁₁ retains the *C*_{2*v*} symmetry framework. The X-ray structure of [B₁₁H₁₀SMe₂]⁻ is compared with the calculated B–B distances in B₁₁H₁₁²⁻, B₁₁H₁₁⁻, and B₁₁H₁₁ in Table 4. Good agreement is found between the X-ray parameters and the dianion. As electrons are removed, the largest change is the lengthening of the *b* and *d* distances and the shortening of the *e* distance. The calculated changes are in moderate agreement with bond index changes¹² calculated with a CNDO-based molecular orbital method.³⁷

The B₁₁H₁₁²⁻ dianion is known to be fluxional, which has been rationalized by a series of degenerate single DSD steps from the *C*_{2*v*} minimum.³⁸ Lipscomb and co-workers³⁸ calculated the *C*_s-symmetry transition state at the PRDDO level and estimated the barrier to be less than 3 kcal/mol. At the current level of theory, the barrier is only 2.0 kcal/mol (B3LYP/6-311+G(d)//B3LYP/6-31G(d)+ZPC). We also calculated the *C*_s transition state for the radical anion and neutral B₁₁H₁₁ species

to determine whether these species (if made) would be fluxional. The rearrangement activation barrier is 3.2 kcal/mol for B₁₁H₁₁⁻ and 6.0 kcal/mol for B₁₁H₁₁ (B3LYP/6-311+G(d)//B3LYP/6-31G(d)+ZPC, both small enough to predict that these species will be fluxional).

B₁₂H₁₂. Using the procedure found above, we found a minimum for a B₁₂H₁₂⁻ ²A_g state of *T_h* symmetry upon removing an electron from B₁₂H₁₂²⁻. The approximate distortion from an icosahedron can be visualized as moving two boron atoms off the 5-fold axis in opposite directions. The unpaired spin density is delocalized on boron atoms over the entire cage. In the isoelectronic radical system, CB₁₁H₁₂, the unpaired spin density was localized on the hemisphere opposite to the carbon atom.²⁵

When the neutral B₁₂H₁₂ cage was optimized in *T_h* symmetry, the calculated force constants revealed three imaginary frequencies. Further optimization eventually resulted in a minimum of *C*_{2*v*} symmetry 10.0 kcal/mol lower in energy than the *T_h* structure. During the optimization from the neutral *T_h* structure to the *C*_{2*v*} structure (*T_h* → *C_s*; then symmetrized to *C*_{2*v*}), two nonadjacent boron atoms in the top tier of five boron atoms became bonded, forcing the intervening boron atom to a position between the two tiers (Figure 1). The capping principle applies but with a slight variation. The *C*_{2*v*} B₁₂H₁₂ structure is a capped version of the B₁₁H₁₁ transition state! The capping BH²⁺ group stabilizes the open face of the B₁₁H₁₁²⁻ *C*_{2*v*} transition state to the point that it is a minimum on the B₁₂H₁₂ PES.

Earlier computations on B₁₂H₁₂ used a local density functional approximation (LDA) with a double- ζ basis set to optimize a cage with *D*_{2*h*} symmetry.³⁹ Using this structure, vertical electron affinities were calculated³⁹ for attaching one electron to form B₁₂H₁₂⁻ (EA₁ = 137.9 kcal/mol) and then a second electron to form B₁₂H₁₂²⁻ (EA₂ = 32.2 kcal/mol). The *D*_{2*h*} structure differs from the *C*_{2*v*} structure in that the top “diamond” of the *C*_{2*v*} structure (see right-hand view of *C*_{2*v*} in Figure 1) has undergone a DSD step with respect to the bottom “diamond”. More recently, HF/6-31G(d) calculations were reported for *D*_{2*h*}, *D*_{3*d*}, and *D*_{5*d*} symmetry structures of B₁₂H₁₂ as models for β -rhombohedral boron.⁴⁰

B₁₃H₁₃. The B3LYP/6-31G(d)-optimized geometry of B₁₃H₁₃²⁻ has been reported recently.¹⁶ The B₁₃H₁₃⁻ radical anion ²B₂ state, derived from the dianion by removing an electron from the HOMO, is calculated to be a minimum at B3LYP/6-31G(d). When an additional electron is removed, the boron atom on the 2-fold axis becomes part of a three-membered BBB bridge and the two flanking terminal hydrogens adopt bridging positions. Clearly, the driving force is the formation of the 12-vertex icosahedral cage. The *C*_{2*v*} structure has one imaginary frequency and relaxes to a structure of *C_s* symmetry in which the bridging boron atom bends to a capping position. While the *C_s* structure was confirmed to be a minimum at the B3LYP/6-31G(d) level, the related *C*_{3*v*} geometry also proved a B3LYP/6-31G* minimum, only 0.2 kcal/mol higher than the *C_s* structure at B3LYP/6-311+G(d)//B3LYP/6-31G(d) + ZPE. This *C*_{3*v*} structure is the fourth member of the 3*p* + 1 *p*-vertex cage series (other members: B₄H₄, B₇H₇, B₁₀H₁₀) whose stability can be understood in terms of the pairing principle as well as the capping principle. The very unusual arrangement of the BH²⁺ cap allows the formation of three additional hydrogen bridging interactions and, more importantly, B₁₃H₁₃ retains the enhanced stabilization (aromaticity, see below) of the B₁₂H₁₂²⁻ cage.

B₁₆H₁₆, B₁₉H₁₉, and B₂₂H₂₂. Three additional 3*p* + 1 *p*-vertex cages have been computed (Figure 2): B₁₆H₁₆ (*T_d*), B₁₉H₁₉ (*C*_{3*v*}),

(37) Armstrong, D. R.; Perkins, P. G.; Stewart, J. J. P. *J. Chem. Soc. A* **1971**, 3674.

(38) Kleier, D. A.; Dixon, D. A.; Lipscomb, W. N. *Inorg. Chem.* **1978**, *17*, 166.

(39) Quong, A. A.; Pederson, M. R.; Broughton, J. Q. *Phys. Rev. B* **1994**, *50*, 4787.

(40) Fujimori, M.; Kimura, K. *J. Solid State Chem.* **1997**, *133*, 178.

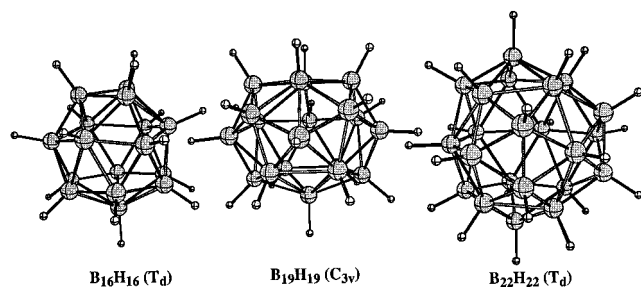
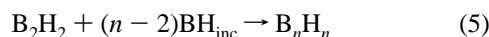
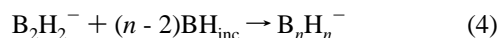
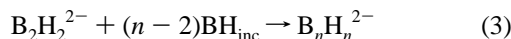


Figure 2. Molecular plots of the three neutral boron hydrides, $B_{16}H_{16}$, $B_{19}H_{19}$, and $B_{22}H_{22}$.

and $B_{22}H_{22}$ (T_d). While optimizations have not been carried out for alternative geometries, the only tendency to add a BH^{2+} cap to the next smaller *closo* cage is found for $B_{16}H_{16}$. This is probably because the nonideal angular arrangement in the capping group is not compensated for by “extra” stabilization of the next smaller *closo* cage. These three $3p + 1$ neutral boron hydride cages ($B_{16}H_{16}$, $B_{19}H_{19}$, and $B_{22}H_{22}$) have been recognized as special by Lipscomb and co-workers,^{41,42} who predicted that the three cages should be stable as the neutral species rather than the dianions. Also, Fowler,³⁰ using Stone’s tensor surface harmonic (TSH) theory, was able to show that “these three clusters have an ‘intrinsic’ departure from the $(n + 1)$ rule.”

General Trends. A number of papers have considered stability trends in the boron hydride dianions.^{16,43–46} A measure of the cage stabilization is given in eqs 3–5, where BH_{inc} is taken as the difference between B_3H_5 (C_{2v} planar) and B_2H_4 (D_{2h} ethylene-like), and $B_2H_2^x$ ($x = -2, -1, 0$) is assumed to have an acetylene-like structure ($D_{\infty h}$ symmetry).⁴⁶



The BH increment is derived from species in which there is no inherent hyperconjugation or delocalization. When normalized by the number of vertices in the cage, energies from eq 3–5 give an indication of the stabilizing effect due to incorporation into the cage (Figures 3–5). From the plot of normalized stabilization in the dianion (Figure 3, see ref 16), there is a clear trend toward increasing stabilization until the 12-vertex cage is reached. In addition, there are dips at $n = 6, 10,$ and 14 . The two smaller cages ($n = 6$ and 10) often have been associated with enhanced stabilization. For the radical anions (Figure 4), there is an overall trend of increased stabilization until the 12-vertex cage. The eight- and nine-vertex cages fall slightly below the trend line. As mentioned above, $B_8H_8^{-}$ has been observed experimentally.²⁰ The data for neutral boron hydrides extend from the five-vertex cage to the 22-vertex cage (Figure 5).

(41) Lipscomb, W. N.; Massa, L. *Inorg. Chem.* **1992**, *31*, 2297.

(42) Derecskei-Kovacs, A.; Dunlap, B. I.; Lipscomb, W. N.; Lowrey, A.; Marynick, D. S.; Massa, L. *Inorg. Chem.* **1994**, *33*, 5617.

(43) Housecroft, C. E.; Snaith, R.; Moss, K.; Mulvey, R. E.; O’Neill, M. E.; Wade, K. *Polyhedron* **1985**, *4*, 1875.

(44) Takano, K.; Izuho, M.; Hosoya, H. *J. Phys. Chem.* **1992**, *96*, 6962.

(45) Schleyer, P. v. R.; Subramanian, G.; Jiao, H.; Najafian, K.; Hofmann, M. In *Advances in Boron Chemistry*; Siebert, W., Ed.; Royal Society of Chemistry: Cambridge, 1997; pp 1–14.

(46) (a) Minkin, V. I.; Glukhovtsev, M. N.; Simkin, B. Y. *Aromaticity and Antiaromaticity*; Wiley: New York, 1994. (b) Schleyer, P. v. R.; Najafian, K. Are Polyhedral Boranes, Carboranes, and Carbocations Aromatic? In *The Borane, Carborane, Carbocation Continuum*; Casanova, J., Ed.; Wiley: New York, 1998; pp 169–190. (c) Schleyer, P. v. R.; Najafian, K. *Inorg. Chem.* **1998**, *37*, 3454.

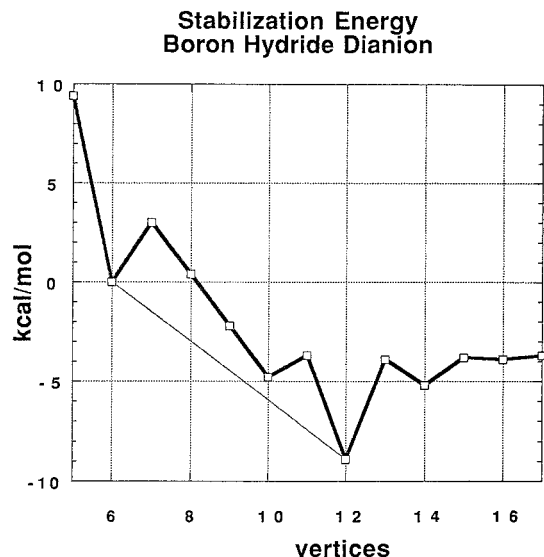


Figure 3. Plot of stabilization energy (defined in eq 3) versus number of vertex boron atoms in dianion cages. The $B_6H_6^{2-}$ and $B_{12}H_{12}^{2-}$ dianions show enhanced stabilization.

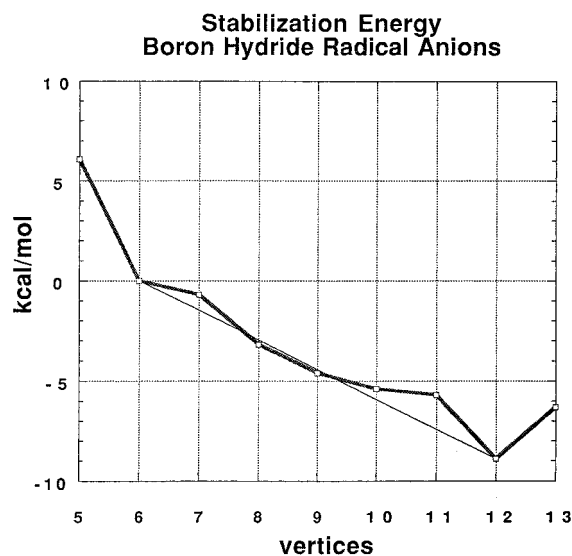


Figure 4. Plot of stabilization energy (defined in eq 4) versus number of vertex boron atoms in radical anion cages. The $B_8H_8^{-}$ and $B_9H_9^{-}$ anions show slightly enhanced stabilization.

Unlike the dianion and radical anion results, the greatest stabilization in the neutral boron hydrides occurs for the 13-vertex cage with slightly increased stability for the seven- and nine-vertex cages. The displacement by one of the minima is due to the capping principle. For the n electron count cages, there is a tendency to form the $n - 1$ deltahedral cage with a BH^{2+} capping group. Thus, the neutral 13-vertex cage can be viewed as the $B_{12}H_{12}^{2-}$ cage capped by a BH^{2+} group. Likewise, the neutral B_7H_7 cage is stabilized by the $B_6H_6^{2-}$ cage with a BH^{2+} group.

Other indicators of cage stability are the average energy and the disproportionation energy (Table 5). The average energy is the total energy divided by the number of vertices relative to a reference ($B_6H_6^n$, $n = 0, -1, -2$). With few exceptions, the average energy reaches a maximum for the 12-vertex cage and levels off at a constant value for larger cages. The disproportionation energy is the energy requirement for a cage to transform into the next larger and the next smaller cages (eq 6).

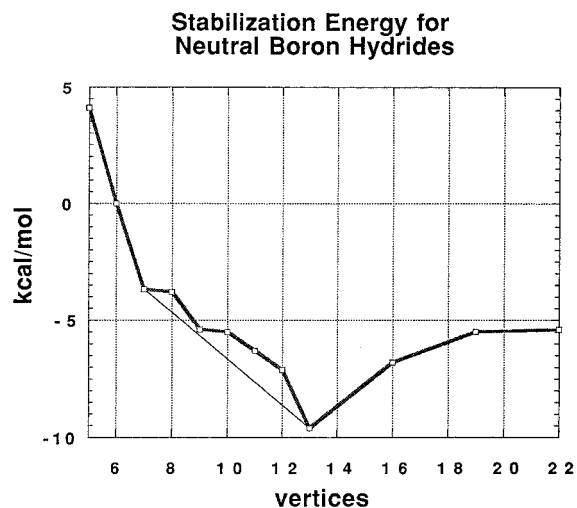
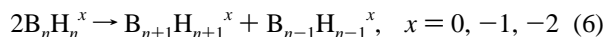


Figure 5. Plot of stabilization energy (defined in eq 5) versus number of vertex boron atoms in neutral cages. The B₇H₇, B₉H₉, and B₁₃H₁₃ boron hydrides show enhanced stabilization.

Table 5. Average Energy (kcal/mol) Relative to Six-Vertex Cage and Disproportionation Energy (kcal/mol) for B_nH_n^x (x = 0, -1, -2) Species at the B3LYP/6-311+G(d)//B3LYP/6-31G(d) Level

	average energy ^a			disproportionation energy ^b			
	neutral	anion	dianion	neutral	anion	dianion	average ^c
B ₅ H ₅	5.6	6.1	12.5				
B ₆ H ₆	0.0	0.0	0.0	-5.4	25.5	41.5	18.0
B ₇ H ₇	-4.8	-0.7	-3.0	21.3	-16.4	6.4	13.8
B ₈ H ₈	-5.7	-3.3	-4.5	-13.1	5.9	-15.2	-14.2
B ₉ H ₉	-7.9	-4.6	-7.3	11.2	2.8	-13.7	-1.2
B ₁₀ H ₁₀	-8.5	-5.4	-11.0	-7.4	3.8	35.2	13.9
B ₁₁ H ₁₁	-9.7	-5.7	-10.7	-2.0	-25.0	-72.6	-35.3
B ₁₂ H ₁₂	-10.8	-8.9	-16.6	-23.6	67.8	121.0	48.7
B ₁₃ H ₁₃	-13.6	-6.3	-12.2			-77.2	
B ₁₄ H ₁₄			-14.0			37.5	
B ₁₅ H ₁₅			-13.1			-21.0	
B ₁₆ H ₁₆	-11.5		-13.6			5.3	
B ₁₇ H ₁₇			-13.7				
B ₁₉ H ₁₉	-10.7						
B ₂₂ H ₂₂	-11.0						

^a Average energy: $AE = 1/6(B_6H_6^c) - 1/n(B_nH_n^c)$, where n is the number of vertices and c is the charge. ^b Disproportionation energy: $DE = B_{n+1}H_{n+1}^c + B_{n-1}H_{n-1}^c - 2B_nH_n^c$, where n is the number of vertices and c is the charge. ^c Average of neutral and dianion disproportionation energies.



A plot of dianion disproportionation energies (Figure 6) clearly reveals the enhanced stability of the 12-vertex dianion (positive values indicate stability of cage to disproportionation). In addition, there are significant peaks for the 10-vertex and the 14-vertex dianions. This suggests that the *closo* 14-vertex dianion is a viable synthetic target. It is also interesting to note that the average of the neutral and dianion disproportionation energies (Table 5) appears to be a predictor of the radical anion disproportionation energies, at least for the larger cages. Thus, the electronic structure of the radical anions appears to be intermediate between those of the corresponding neutral and dianion cages.

We have calculated HOMO–LUMO gaps (see Figure 7) and vertical ionization potentials (B3LYP/6-311+G(d)//B3LYP/6-31G(d)) from the fixed dianion geometries ($B_nH_n^{2-} \rightarrow B_nH_n^-$ and $B_nH_n^{2-} \rightarrow B_nH_n$, $n = 5–17$; the geometries for $B_nH_n^{2-}$, $n = 13–17$, were taken from ref 16). A plot of the HOMO–LUMO gaps shows maxima which indicate enhanced stability

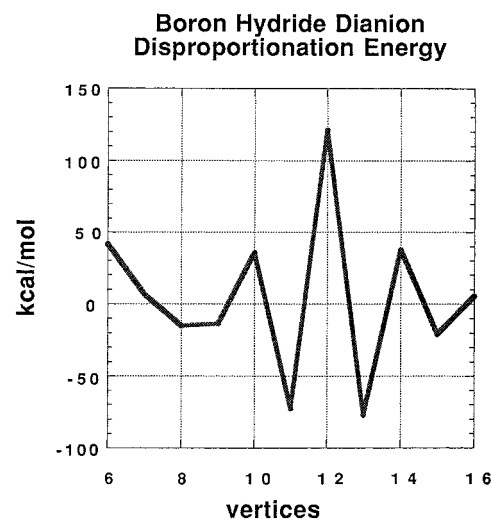


Figure 6. Plot of disproportionation energy (kcal/mol) (defined in eq 6) versus number of vertex boron atoms in dianion cages. Note the larger values for cage sizes of $n = 10, 12,$ and 14 .

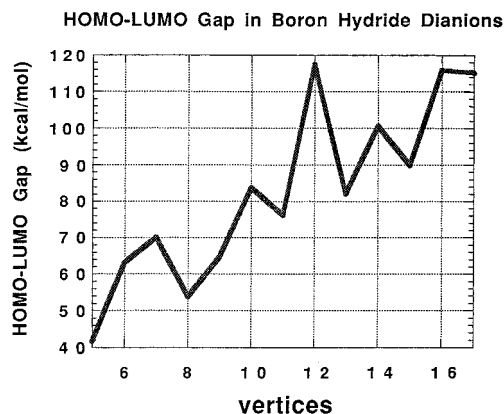


Figure 7. Plot of HOMO–LUMO gap (kcal/mol) versus number of vertex boron atoms in dianion cages. Note the larger values for cage sizes of $n = 7, 10, 12,$ and 14 .

Table 6. HOMO–LUMO Gap (kcal/mol) and Vertical and Adiabatic Ionization Potentials (kcal/mol) for Boron Hydride Dianions Calculated at the B3LYP/6-311+G(d)//B3LYP/6-31G(d) Level

	vertical IP		adiabatic IP ^a		
	H–L gap	-2 → -1	-2 → 0	-2 → -1	-2 → 0
B ₅ H ₅ ²⁻	41.6	-60.0	28.0	-66.4 (6.4)	-10.4 (38.4)
B ₆ H ₆ ²⁻	63.1	-34.5	107.3	-40.9 (6.4)	29.0 (78.3)
B ₇ H ₇ ²⁻	70.0	-23.1	98.0	-31.5 (8.4)	21.4 (76.6)
B ₈ H ₈ ²⁻	53.8	-39.0	53.7	-44.8 (5.8)	28.8 (24.9)
B ₉ H ₉ ²⁻	64.7	-27.6	74.5	-36.9 (9.3)	38.3 (36.2)
B ₁₀ H ₁₀ ²⁻	83.7	-6.1	117.0	-12.6 (6.5)	72.6 (44.4)
B ₁₁ H ₁₁ ²⁻	76.1	-12.4	97.3	-19.7 (7.3)	64.3 (33.0)
B ₁₂ H ₁₂ ²⁻	117.4	37.7	184.2	10.9 (26.8)	126.7 (57.5)
B ₁₃ H ₁₃ ²⁻	82.1	-3.7	108.9	-11.7 (8.0)	44.7 (64.2)
B ₁₄ H ₁₄ ²⁻	100.5	14.3	138.2		
B ₁₅ H ₁₅ ²⁻	89.8	5.4	120.2		
B ₁₆ H ₁₆ ²⁻	115.8	30.7	165.1		110.1 (55.0)
B ₁₇ H ₁₇ ²⁻	115.1	31.5	167.8		

^a Number in parentheses is the energy lowering (kcal/mol) caused by geometry optimization.

at $n = 7, 10, 12,$ and 14 . Table 6 tabulates vertical ($n = 5–17$) and adiabatic ($n = 5–13$) ionization potentials. These are plotted in Figure 8. The two curves track each other closely; the adiabatic curve (Figure 8) is about 6–9 kcal/mol lower in energy. These results show that B₁₂H₁₂²⁻ is the smallest *closo* boron hydride dianion which can overcome Coulomb repulsion;

Table 7. Calculated Unpaired Spin Density at the B3LYP/6-311+G(d) Level for Boron Hydride Radical Anions^a

	PG (ES)	"a"	"b"	"c"	"d"	"e"	"f"	total α^b
B ₅ H ₅ ⁻	C _{4v}	0.372 (1)	0.388 (2)	-0.038 (2)				1.15
B ₆ H ₆ ⁻	D _{3d}	0.176 (6)						1.06
B ₇ H ₇ ⁻	C _s (² A'')	-0.016 (2)	0.282 (1)	0.035 (1)	-0.004 (1)	0.231 (1)	0.379 (1)	0.93
B ₈ H ₈ ⁻	D _{2d}	0.027 (4)	0.217 (4)					0.98
B ₉ H ₉ ⁻	D _{3h}	0.052 (6)	0.252 (3)					1.07
B ₁₀ H ₁₀ ⁻	C _{2v}	0.330 (1)	0.068 (4)	-0.058 (2)	0.156 (2)	0.247 (1)		1.16
B ₁₁ H ₁₁ ⁻	C _{2v}	-0.055 (1)	0.015 (2)	0.055 (2)	0.208 (2)	0.113 (4)		1.01
B ₁₂ H ₁₂ ⁻	T _h	0.090(12)						1.08
B ₁₃ H ₁₃ ⁻	C _{2v}	0.266(1)	0.126(2)	-0.024(2)	0.084(4)	0.040(2)	0.005(2)	0.94

^a The unpaired spin density is given for the boron atoms labeled in Figure 1. The number in parentheses is the number of equivalent boron positions. ^b Total α spin on boron vertexes.

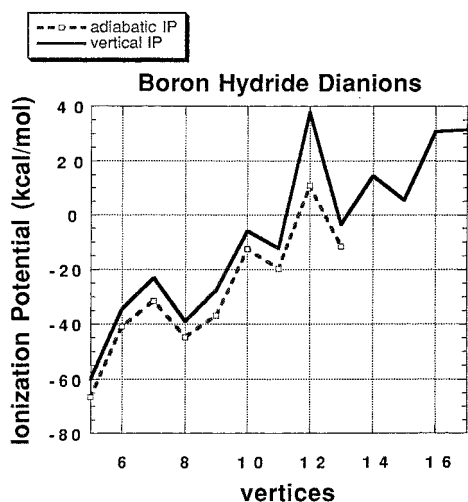


Figure 8. Plot of ionization potential (kcal/mol) for removing the first electron of the dianion (B_nH_n²⁻ → B_nH_n⁻). The solid line represents vertical ionization potentials and the dashed line adiabatic ionization potentials.

thus, it is thermodynamically stable in the gas phase, with an ionization potential of 10.9 kcal/mol (0.47 eV). Indeed, it is possible to observe the B₁₂H₁₂²⁻ dianion^{47a} (as well as B₁₀H₁₀²⁻) in the gas phase using electrospray mass spectrometry^{47b} to study the icosahedral dianion in the gas phase. Since the vertical ionization of B₁₄H₁₄²⁻ is 14.3 kcal/mol (0.62 eV), this dianion also should have a measurable lifetime in the gas phase. However, it is not yet clear whether geometry optimization of the radical anion will lead to an endothermic (bound) or exothermic (unbound) adiabatic ionization potential for the B₁₄H₁₄²⁻ dianion.⁴⁸ The dianion cages B₁₆H₁₆²⁻ and B₁₇H₁₇²⁻ have even larger vertical ionization potentials of 30.7 kcal/mol (1.33 eV) and 31.5 kcal/mol (1.36 eV), respectively; they should have adiabatic stability as well.

In Figure 9, we have plotted the HOMO–LUMO gaps for neutral boron hydrides, B_nH_n, $n = 5–13$. The validity of the pairing principle is clearly evident. There are large increases in the HOMO–LUMO gaps for $3p + 1$ p -vertex cages, B₇H₇, B₁₀H₁₀, and B₁₃H₁₃. We have not computed the intervening boron hydrides between the 13-, 16-, and 22-vertex species. It would be interesting to see if the larger $3p + 1$ neutral boron hydrides also had greater HOMO–LUMO gaps compared to their neighbors.

Unpaired spin densities are given for the most stable radical anions in Table 7. The column labels (“a”–“f”) refer to the

(47) (a) Hop, C. E. C. A.; Saulys, D.; Gaines, D. F. *Inorg. Chem.* **1995**, *34*, 1977. (b) Kebarle, P.; Tang, L. *Anal. Chem.* **1993**, *65*, 272A and references therein.

(48) For a discussion of dianions with unbound electrons, see: Sommerfeld, T.; Schneller, M. K.; Cederbaum, L. S. *J. Chem. Phys.* **1995**, *103*, 1057.

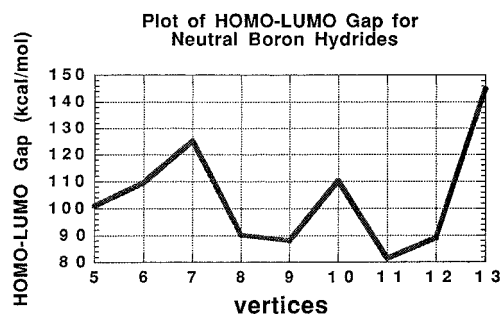


Figure 9. Plot of HOMO–LUMO gap (kcal/mol) versus number of vertex boron atoms in neutral cages. Note the larger values for cage sizes of $n = 7, 10$, and 13 .

vertex labels in Figure 1; the column labeled “total α ” refers to the sum of α spins on all boron atoms. A value less than 1.00 would indicate unpaired spin density on hydrogen atoms, while a value greater than 1.00 would indicate that β spin density is present on boron and/or hydrogen atoms (spin polarization). For most radical anions, the unpaired spin density is distributed to only about half of the boron atoms. Two exceptions are B₆H₆⁻ and B₁₂H₁₂⁻, in which equal spin densities are enforced by symmetry.

Three-Dimensional Aromaticity of Neutral and Radical Monoanion Boron Hydrides. Conventionally, aromaticity is often discussed in term of various criteria such as energetic (resonance and aromatic stabilization energies ASE), magnetic (¹H NMR chemical shifts, magnetic susceptibility anisotropies and their exaltations, and NICS), and geometric (bond length equalization).^{45,46,49} NICS (nucleus-independent chemical shift), proposed by Schleyer and co-workers,⁴⁹ is defined as the negative of the absolute magnetic shieldings computed, e.g., at or above the geometrical centers of rings or clusters. Negative NICS values at those positions indicate aromaticity (diatropic ring currents), and positive values indicate antiaromaticity (paratropic ring currents). The effectiveness of NICS as a simple and efficient criterion to probe two- and three-dimensional delocalization has been demonstrated by studies on the wide-ranging sets of two- and three-dimensional aromatic compounds.^{46,47,49} Therefore, NICS values were computed for neutral and radical monoanion boron hydrides at the GIAO-HF/6-31+G(d) and GIAO-B3LYP/6-31+G(d) levels using B3LYP/6-31G(d) geometries (Table 8) to study their three-dimensional

(49) (a) Hofmann, M.; Schleyer, P. v. R. *Inorg. Chem.* **1999**, *38*, 652. (b) Schleyer, P. v. R.; Maerker, C.; Dransfeld, A.; Jiao, H.; Hommes, N. J. R. v. E. *J. Am. Chem. Soc.* **1996**, *118*, 6317. (c) Jiao, H.; Schleyer, P. v. R. *Angew. Chem., Int. Ed. Engl.* **1996**, *35*, 2383. (d) Schleyer, P. v. R.; Jiao, H. *Pure Appl. Chem.* **1996**, *68*, 209. (e) Subramanian, G.; Schleyer, P. v. R.; Jiao, H. *Angew. Chem., Int. Ed. Engl.* **1996**, *35*, 2638. (f) Unverzagt, M.; Winkler, H. J.; Brock, M.; Hofmann, M.; Schleyer, P. v. R.; Massa, W.; Berndt, A. *Angew. Chem., Int. Ed. Engl.* **1997**, *36*, 853. (g) Schleyer, P. v. R.; Jiao, H.; Hommes, N. J. R. v. E. *J. Am. Chem. Soc.* **1997**, *119*, 12669. (h) Schleyer, P. v. R.; Najafian, K. *Inorg. Chem.* **1998**, *37*, 3454.

Table 8. Nucleus-Independent Chemical Shifts (NICS) for Dianionic, Neutral, and Monoanion Boron Hydrides (in ppm)

PG	ES	NICS ^a	NICS ^{b,c}	NICS(1) ^c	
Dianion					
B ₅ H ₅ ²⁻	D _{3h}	¹ A ₁ '	-26.5	-24.6	-16.1
B ₆ H ₆ ²⁻	O _h	¹ A _{1g}	-34.3	-29.9	-14.0
B ₇ H ₇ ²⁻	D _{5h}	¹ A ₁ '	-27.5	-20.9	-13.3
B ₈ H ₈ ²⁻	D _{2d}	¹ A ₁	-24.2	-18.1	-9.6, -13.1
B ₉ H ₉ ²⁻	D _{3h}	¹ A ₁ '	-27.4	-21.8	-11.6, -15.2
B ₁₀ H ₁₀ ²⁻	D _{4d}	¹ A ₁	-33.5	-29.3	-12.6, -11.1
B ₁₁ H ₁₁ ²⁻	C _{2v}	¹ A ₁	-32.5	-26.7	-10.8, -10.6, -9.7, -20.4
B ₁₂ H ₁₂ ²⁻	I _h	¹ A _g	-35.8	-28.3	-9.5
B ₁₃ H ₁₃ ²⁻	C _{2v}	¹ A ₁	-30.9	-23.3	-10.1, -10.5, -9.0, -8.9, -9.4
B ₈ H ₈ ²⁻	C _{2v}	¹ A ₁	-20.1	-14.7	-13.4, -12.9, -12.5, -10.6, -9.1
B ₁₁ H ₁₁ ²⁻	C _s	¹ A ₁ '	-31.8	-26.1	-14.1, -11.7, -11.2, -10.2, -9.9, -9.9, -9.8, -9.3, -8.8, -8.4
Neutral					
B ₅ H ₅	C _{4v}	¹ A ₁	41.8	27.4	-5.3, -18.2
B ₆ H ₆	C _{2v}	¹ A ₁	-10.6	-17.4	-19.1, -11.0, -12.3
B ₇ H ₇	C _{3v}	¹ A ₁	-13.6	-11.7	-13.4, -10.0, -10.5, -10.0, -0.3
B ₈ H ₈	C _{2v}	¹ A ₁	14.6	12.9	-4.8, -5.3, -8.1, -5.7, -9.4
B ₈ H ₈	D _{2d}	¹ A ₁	12.3	9.5	-7.7, -5.4
B ₉ H ₉	C _{4v}	¹ A ₁	27.3	27.2	-6.7, -7.6, -2.3, -11.6
B ₉ H ₉	D _{3h}	¹ A ₁ '	29.3	28.1	-5.6, -3.4, -8.3
B ₁₀ H ₁₀	C _{3v}	¹ A ₁	10.4	5.6	-6.7, -10.9
B ₁₁ H ₁₁	C _s	¹ A ₁ '	7.8	2.1	-7.6, -8.5, -7.4, -7.9, -4.5, -10.9, -8.6, -1.5, -9.5, -9.7
B ₁₁ H ₁₁	C _{2v}	¹ A ₁	1.8	-4.7	-8.1, -9.0, -11.9, -6.0, -11.8
B ₁₂ H ₁₂	T _h	¹ A _g	69.2	74.4	-3.9, -10.7
B ₁₂ H ₁₂	C _{2v}	¹ A ₁	-11.0	-12.4	-3.7, -7.2, -7.9, -10.6, -8.7
B ₁₃ H ₁₃	C _{3v}	¹ A ₁	-30.0	-21.8	-11.7, -10.7, -10.0, -8.4, -7.8
B ₁₃ H ₁₃	C _{2v}	¹ A ₁	-28.4	-20.1	-29.6, -25.5, -10.8, -9.8, -10.5, -8.5, -7.8, -7.5
B ₁₃ H ₁₃	C _s	¹ A ₁ '	-29.8	-21.6	-11.8, -11.7, -11.5, -10.3, -0.0, -9.9, -9.6, -8.6, -8.4, -8.1, -7.9, -7.9, -7.6
B ₁₆ H ₁₆	T _d	¹ A ₁	21.4	23.1	
B ₁₉ H ₁₉	C _{3v}	¹ A ₁	1.4	-0.5	
B ₂₂ H ₂₂	T _d	¹ A ₁	1.8	2.4	
Radical Monanion					
B ₅ H ₅ ⁻	C _{2v}	² B ₁	12.8	16.9	
B ₅ H ₅ ⁻	C _{2v}	² A ₂	12.5	16.5	
B ₆ H ₆ ⁻	D _{2h}	² B _{3g}	42.7	67.5	
B ₆ H ₆ ⁻	D _{3d}	² A _{1g}	43.4	49.5	
B ₇ H ₇ ⁻	C _s	² A ₁ '	-16.9	-13.2	
B ₇ H ₇ ⁻	C _s	² A ₂ '	-14.2	-9.8	
B ₈ H ₈ ⁻	C _{2v}	² B ₁	-2.1	1.3	
B ₈ H ₈ ⁻	D _{2d}	² A ₁	-6.8	-3.3	
B ₉ H ₉ ⁻	D _{3h}	² A ₁ '	-0.9	4.2	
B ₁₀ H ₁₀ ⁻	D ₂	² B ₁	4.9	14.2	
B ₁₀ H ₁₀ ⁻	C _{2v}	² B ₁	4.4	13.6	
B ₁₁ H ₁₁ ⁻	C _{2v}	² A ₁ '	-10.9	-8.8	
B ₁₁ H ₁₁ ⁻	C _s	² A ₂	-11.2	-7.0	
B ₁₂ H ₁₂ ⁻	T _h	² A _u	31.4	46.7	
B ₁₃ H ₁₃ ⁻	C _{2v}	² B ₂	-21.6	-13.3	

^a NICS at the geometric centers, calculated at the HF/6-31+G* level.^b NICS at the geometric centers, calculated at the B3LYP/6-31+G* level. ^c NICS for the points 1.0 Å above the unique triangles, calculated at the B3LYP/6-31+G* level.

aromaticity. The GIAO-B3LYP/6-31+G(d)//B3LYP/6-31G(d) results will be used in the discussions below.

The three-dimensional delocalization of *closo* borane dianions was the subject of several papers.^{46,47,49-53} The conclusion that they exhibit three-dimensional aromaticity was supported by the large negative NICS computed at geometrical centers between -25 and -35 ppm (GIAO-HF/6-31+G(d)//B3LYP/6-31G(d)).^{49h} Although the NICS values (see Table 8) at the DFT GIAO-B3LYP/6-31+G(d) level are somewhat lower in

magnitude, the previous conclusions remain unchanged. The NICS for the new C_{2v} B₈H₈²⁻ structure is -14.7 ppm, which can be compared to -18.1 ppm for the more stable D_{2d} structure. The new C_s B₁₁H₁₁²⁻ has a NICS value of -26.1 ppm, which is close to that for the C_{2v} structure. In Table 8, NICS data are included for points 1.0 Å above each unique triangle. All these NICS values are negative with values between -9.0 and -20.4 ppm. Thus, the diatropic effect of three-dimensional aromaticity extend outside the cages, as well as being exhibited inside. This is not like the case for benzene with its well-known shielding and deshielding regions.

Removing two electrons from the *closo* borane dianions gives the neutral boron hydrides. Qualitatively, it is reasonable to expect that the neutral boron hydrides should be more reactive and less stable if the HOMOs in the *closo* borane dianions are degenerate. As shown in Table 8, the *closo* borane dianions all have negative NICS values between -18.0 and -29.9 ppm. In contrast, most neutral boron hydrides have positive (antiaromatic) NICS values or very small values. The compounds mentioned below are exceptions. In particular, B₁₃H₁₃ is the most aromatic among the neutral boron hydrides studied here, and the NICS values (about -21.0 ppm) for the three structures with different symmetries (C_{3v}, C_{2v}, and C_s) are comparable to the NICS values for B₁₃H₁₃²⁻ (-23.3 ppm). It should be pointed out that B₁₃H₁₃²⁻ has no degenerate HOMOs and B₁₃H₁₃ meets the capping and pairing principles. Also, B₁₃H₁₃ is the most stable neutral species in our set in terms of average energy and disproportion energy criteria (see above). For B₁₂H₁₂, the lower symmetry and more stable C_{2v} structure has a NICS value of -12.4 ppm (compared to -28.3 ppm for I_h B₁₂H₁₂²⁻). The anomalously large NICS value (74.4 ppm) for the T_h structure (NIMAG = 3) is due to the small HOMO-LUMO gap.⁵⁶ The NICS values of -17.4 and -11.7 ppm for B₆H₆ and B₇H₇ suggest that these neutral boron hydrides are aromatic but less so than the corresponding dianions which have NICS values of -29.9 and -20.9 ppm, respectively. Although neutral boron hydrides have different aromatic character, NICS values for the points 1.0 Å above the unique triangles are all negative, even for the exceptional (most antiaromatic) B₁₂H₁₂ (T_h symmetry) isomer.

The NICS criterion indicates that the B₇H₇⁻, B₁₁H₁₁⁻, and B₁₃H₁₃⁻ radical anions are aromatic (NICS = -7 to -13 ppm); B₅H₅⁻, B₆H₆⁻, B₁₀H₁₀⁻, and B₁₂H₁₂⁻ are antiaromatic (NICS = 14 to 68 ppm); and B₈H₈⁻ and B₉H₉⁻ are nonaromatic (NICS = -3 to 1 ppm). It is perhaps significant that the two most antiaromatic boron hydride monoanions, B₆H₆⁻ and B₁₂H₁₂⁻, also have the greatest delocalization of unpaired spin density (Table 7).

The IGLO method, implemented in the DeMon NMR program,⁵⁴ allows detailed analysis in term of contributions from the individual localized MOs.⁵⁵ The "dissected" NICS values of the neutral and dianionic B₅H₅, B₆H₆, B₇H₇, and B₈H₈ are shown in Figure 10 with the localization given by the Pipek-Mezey algorithm method.⁵⁷ The values indicate the contributions from the electron pair. Because these boron compounds are electron-deficient, the electron pairs may be localized to a subset of chemically equivalent B-B bonds. Such localization schemes

(54) (a) Malkin, V. G.; Malkin, O. L.; Eriksson, L. A.; Salahub, D. R. In *Modern Density Functional Theory*; Seminario, J. M., Politzer, P., Eds.; Elsevier: Amsterdam, 1995; p 273. (b) Malkin, V. G.; Malkin, O. L.; Eriksson, L. A.; Salahub, D. R. *J. Am. Chem. Soc.* **1994**, *116*, 5898.

(55) Kutzelnigg, W.; Fleischer, U.; Schindler, M. In *NMR: Basic Principles and Progress*; Springer: Berlin, 1990; Vol. 23, p 165.

(56) Wiberg, K. B.; Hammer, J. D.; Keith, T. A.; Zilm, K. *J. Phys. Chem. A* **1999**, *103*, 21.

(57) Pipek, J.; Mezey, P. G. *J. Chem. Soc.* **1989**, *90*, 4916.

(50) King, R. B.; Rouvray, D. H. *J. Am. Chem. Soc.* **1977**, *99*, 7834.

(51) Jemmis, E. D.; Schleyer, P. v. R. *J. Am. Chem. Soc.* **1982**, *104*, 4781.

(52) Jemmis, E. D. *J. Am. Chem. Soc.* **1982**, *104*, 7071.

(53) Aihara, J. *J. Am. Chem. Soc.* **1978**, *100*, 3339.

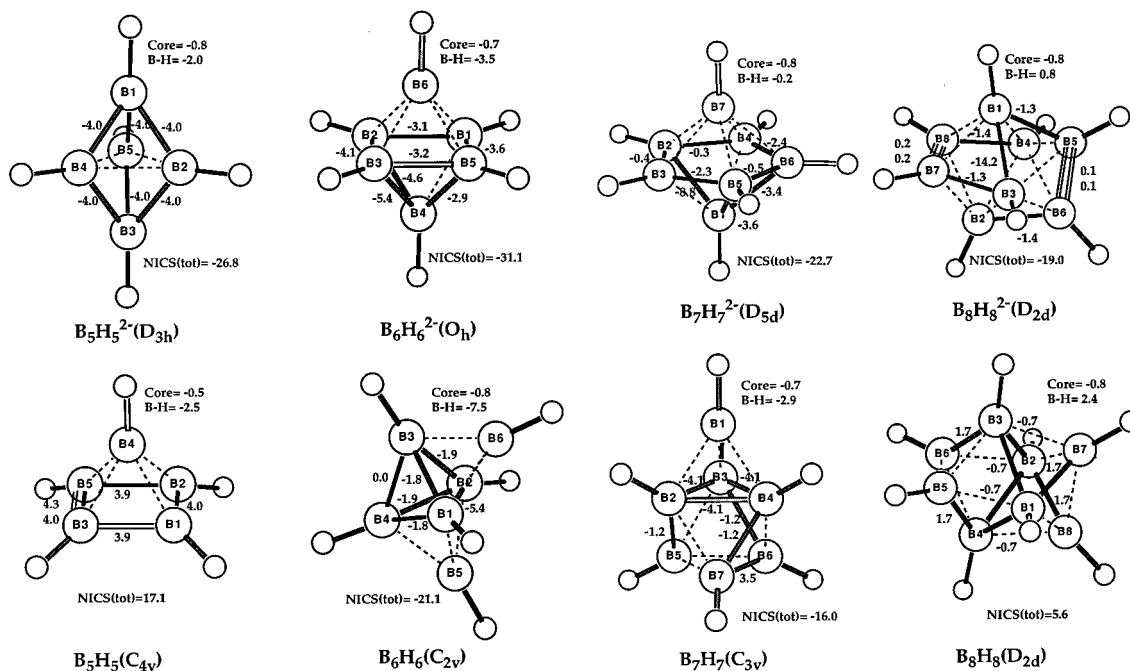


Figure 10. Localization scheme given by the Pipek–Mezey method for dianion and neutral forms of B_5H_5 , B_6H_6 , B_7H_7 , and B_8H_8 . The values above the bonds in the figure indicate the contribution (ppm) from the electron pair to the dissected NICS values. Likewise, the “core” and “B–H” values indicate the contribution (ppm) from the boron 1s electrons and the B–H bonds, respectively, to the dissected NICS values.

can be thought of as individual resonance contributions which, taken together, reproduce the molecular symmetry.

The dissected NICS analyses for neutral and dianionic B_5H_5 and B_8H_8 are examples. In the D_{3h} $B_5H_5^{2-}$ dianion, the localization of the six electron pairs is to the six shortest B–B bonds ($R = 1.676 \text{ \AA}$): each contributes -4.0 ppm. The remaining NICS contributions (-2.8 ppm) come from the 1s boron cores (-0.8 ppm) and from the five B–H bonds (-2.0 ppm). For the neutral C_{4v} B_5H_5 , the five electron pairs localize on the sides of square $B_1B_2B_3B_4$ (two electron pairs localize on the B_1B_3 bond), which makes a 20.0 ppm contribution to the total NICS values of 17.1 ppm. The core and BH bonds contribute -0.5 and -2.5 ppm, respectively. In $B_8H_8^{2-}$ (D_{2d}), the shortest B_5B_6 and B_7B_8 ($R = 1.615 \text{ \AA}$) bonds are assigned four pairs by the localization scheme (double bonds), but their total contribution (0.3 ppm) is negligible. The four 1.707-\AA BB bonds contribute a total of -5.4 ppm to the shielding. This leaves two electrons which can be considered to constitute 4c-2e bonding involving $B_1B_2B_3B_4$. The two electrons are localized artificially to the B_1B_3 bond and contribute most (-14.2 ppm) of the total shielding. The minor paratropic contribution (total 0.8 ppm) of the BH bonds is balanced by those from the boron cores (total -0.8 ppm). Hence, the -19.3 ppm NICS value in the center arises from the delocalized bonding involving $B_1B_2B_3B_4$ (-14.2 ppm) as well as -5.4 ppm from the four adjacent BB bonds. The other contributions are small and also largely cancel. Four of the eight electron pairs in $B_8H_8^{2-}$ (D_{2d}) are assigned to the four longest B–B bonds ($R = 1.925 \text{ \AA}$) which form a $B_1B_2B_3B_4$ unit similar to that in $B_8H_8^{2-}$ (D_{2d}). However, the contribution (-2.8 ppm) from $B_1B_2B_3B_4$ is much less than that (-14.2 ppm) in $B_8H_8^{2-}$ (D_{2d}). The remaining four electron pairs are assigned to the four shortest B–B bonds ($R = 1.742 \text{ \AA}$), which contribute 6.1 ppm to the deshielding (NICS = 5.6 ppm). The four B–H bonds related to the $B_1B_2B_3B_4$ have negative contributions (-1.6 ppm), while other B–H bonds contribute 4.0 ppm. The remaining -0.8 ppm comes from cores.

Conclusions

A survey has been made of the *hypercloso* neutral boron hydrides (B_nH_n , $n = 5-13, 16, 19, 22$) and radical anion boron hydrides ($B_nH_n^-$, $n = 5-13$). The pairing and the capping principles help explain the nature of the neutral cages. Enhanced stability seems to be associated with the $3p + 1 p$ -vertex cages (one boron atom on a 3-fold axis), which is evident from larger HOMO–LUMO gaps and greater stabilization energies. The 13-vertex cage appears to be the most stable neutral boron hydride cage. This prediction can be explained by the fact that the capped geometry enjoys the stabilization of the next smaller *closo* cage, the icosahedral $B_{12}H_{12}^{2-}$ (capping principle).

Dianions which have degenerate HOMOs have radical anion geometries which are distorted owing to the Jahn–Teller theorem. However, the distortions from the dianion geometries are rather small. With the exception of $B_{12}H_{12}^{2-}$, the adiabatic ionization potentials (from the dianion) are only about 6–9 kcal/mol lower in energy than the vertical ionization potentials. $B_{12}H_{12}^{2-}$ is the first dianion which is predicted to overcome Coulomb repulsion between the two negative charges sufficiently to be stable in the gas phase (IP = 0.47 eV). The vertical ionization of $B_{14}H_{14}^{2-}$ (IP = 0.62 eV) indicates that the dianion should have a significant lifetime.

The ESR parameters have been computed for the $B_8H_8^-$ radical anion, which is predicted to undergo rapid rearrangement in a $D_{2d} \rightarrow C_{2v} \rightarrow D_{2d}$ DSD mechanism. $B_{10}H_{10}^-$ and $B_{11}H_{11}^-$ are other radical anions which are predicted to be fluxional.

The negative NICS values of the neutral B_6H_6 (C_{2v}), B_7H_7 (C_{3v}), $B_{12}H_{12}$ (C_{2v}), and $B_{13}H_{13}$ (C_{3v} and C_s) indicate their three-dimensional aromatic character. Among the neutral boron hydrides studied, these $B_{13}H_{13}$ forms have the most negative NICS values and are the most aromatic. This conclusion is consistent with the greater stabilization energy than those for other neutral boron hydrides and the larger HOMO–LUMO gap. Therefore, $B_{13}H_{13}$ is proposed as a good candidate for synthesis.

Acknowledgment. This paper is dedicated with admiration to Professor William N. Lipscomb on the occasion of his 80th birthday. Computer time was provided by the Alabama Super-computer Network. M.L.M. would like to thank Sun Microsystems Computer Corp. for the award of an Academic Equipment Grant.

Supporting Information Available: Tables of absolute energies (hartrees) and zero-point energies (kcal/mol) at the B3LYP/6-31G(d)//B3LYP/6-31G(d) level for neutral, radical

anion, and dianion boron hydrides; absolute energies at the B3LYP/6-311+G(d) level for the dianion, radical anion, and neutral boron hydrides, all evaluated at the dianion B3LYP/6-31G(d)-optimized geometry; and Cartesian coordinates for relevant structures optimized at the B3LYP/6-31G(d) level (PDF). This material is available free of charge via the Internet at <http://pubs.acs.org>.

JA994490A